Available online at www.sciencedirect.com
SciVerse ScienceDirect
Journal of the European Ceramic Society xxx (2012) xxx–xxx
www.elsevier.com/locate/jeurceramsoc

Novel iron oxide–silica coreshell powders compacted by using pulsed electric current sintering: Optical and magnetic properties

N. Mahmed [a,d,*], O. Heczko [b], R. Maki [a,c], O. Söderberg [a], E. Haimi [a], S-P. Hannula [a]

[a] Aalto University School of Chemical Technology, Department of Materials Science and Engineering, P.O. Box 16200, FI-00076 Aalto, Finland
[b] Institute of Physics, Academy of Sciences, Czech Republic Na Slovance 2, CZ-182 21 Praha 8, Czech Republic
[c] Industrial Science and Technology Policy and Environment Bureau, Ministry of Economy, Trade and Industry (METI), Kasumigaseki 1-3-1, Chiyoda-ku, Tokyo 100-8901, Japan
[d] School of Materials Engineering, Kompleks Pusat Pengajian UniMAP, Taman Muhibbah, Universiti Malaysia Perlis, 02600 Jejawi, Perlis, Malaysia

Abstract

The properties of the bulk materials consolidated of silica coreshell powders with iron oxide core have been studied. Iron oxide nanoparticles smaller than 20 nm in size were synthesized by a reverse co-precipitation process in ambient atmosphere. Coreshell structures with various amounts of iron oxide were prepared via a modified Stöber method. The powders were compacted by using pulsed electric current sintering (PECS) at 1373 K. The morphologies, microstructures, phases, optical, and magnetic properties of the samples were studied by using transmission electron microscope (TEM), scanning electron microscope (SEM), X-ray diffraction (XRD), UV–visible spectroscopy (UV–Vis), and vibrating sample magnetometer (VSM). Transmittance values in the 250–800 nm range varied with the amount of iron oxide. Sample with the lower content was transparent while the sample with the highest content was opaque with microporosity. The compact with the highest iron oxide content showed the ferromagnetic behaviour at 300 K. The phase transformations in the coreshell powders during the sintering process are discussed.

Keywords: Sintering; SiO_2; Ferrites; Grain growth; Transparent

1. Introduction

Magnetic nanoparticles such as magnetite (Fe_3O_4), maghemite (γ-Fe_2O_3) and pure iron, Fe are known to exhibit high saturation magnetization values.[1–3] When they are combined with transparent matrix materials, the composites can create novel and potential applications based on their magnetic and optical properties. One of the properties that have attracted much attention in recent research is the magneto-optical effect that can be applied in various fields such as magneto-optical switches, information storage, optical fibre sensors, and optical isolators.[4–6] Several studies deal with preparing transparent magnetic material based on iron oxide particles by using a variety of transparent matrices. Yamaguchi et al.[7] have synthesized the transparent magnetic thin films by embedding Fe_3O_4 nanoparticles into the polyvinyl alcohol (PVA) matrix. However, due to the thermal and chemical instability of the polymer, the silica (SiO_2) matrix has received increasing interest. Yasumori et al.[8] produced a transparent silica gel layer with embedded magnetite nanoparticles by using a sol–gel method, and Thomas et al.[9] reported on crack-free transparent magnetic-silica monoliths, in which the magnetite nanoparticles with various concentrations were entrapped within a sol–gel silica network formed in heat treatment. The magnetic and transparency behaviour of the both type of samples were found to depend on the iron oxide concentrations.

However, there are apparently no reports about sintering of the bulk transparent magnetic material made of the amorphous silica powders with the iron oxide nanoparticle cores particularly by using the pulsed electric current sintering (PECS) method. PECS which also called spark plasma sintering (SPS) or field assisted sintering technique (FAST) applies pulsed direct current and uniaxial pressure to consolidate the powders. This technique has been used for composites,[10] superconductors,[11] and

* Corresponding author at: Aalto University School of Chemical Technology, Department of Materials Science and Engineering, P.O. Box 16200, FI-00076 Aalto, Finland. Tel.: +358 9 47022688; fax: +358 9 47022677.
E-mail addresses: norsuria.mahmed@aalto.fi (N. Mahmed), heczko@fzu.cz (O. Heczko), maki-ryuji@meti.go.jp (R. Maki), outi.soderberg@aalto.fi (O. Söderberg), eero.haimi@aalto.fi (E. Haimi), simo-pekka.hannula@aalto.fi (S-P. Hannula).

0955-2219/$ – see front matter © 2012 Elsevier Ltd. All rights reserved.
doi:10.1016/j.jeurceramsoc.2012.02.050

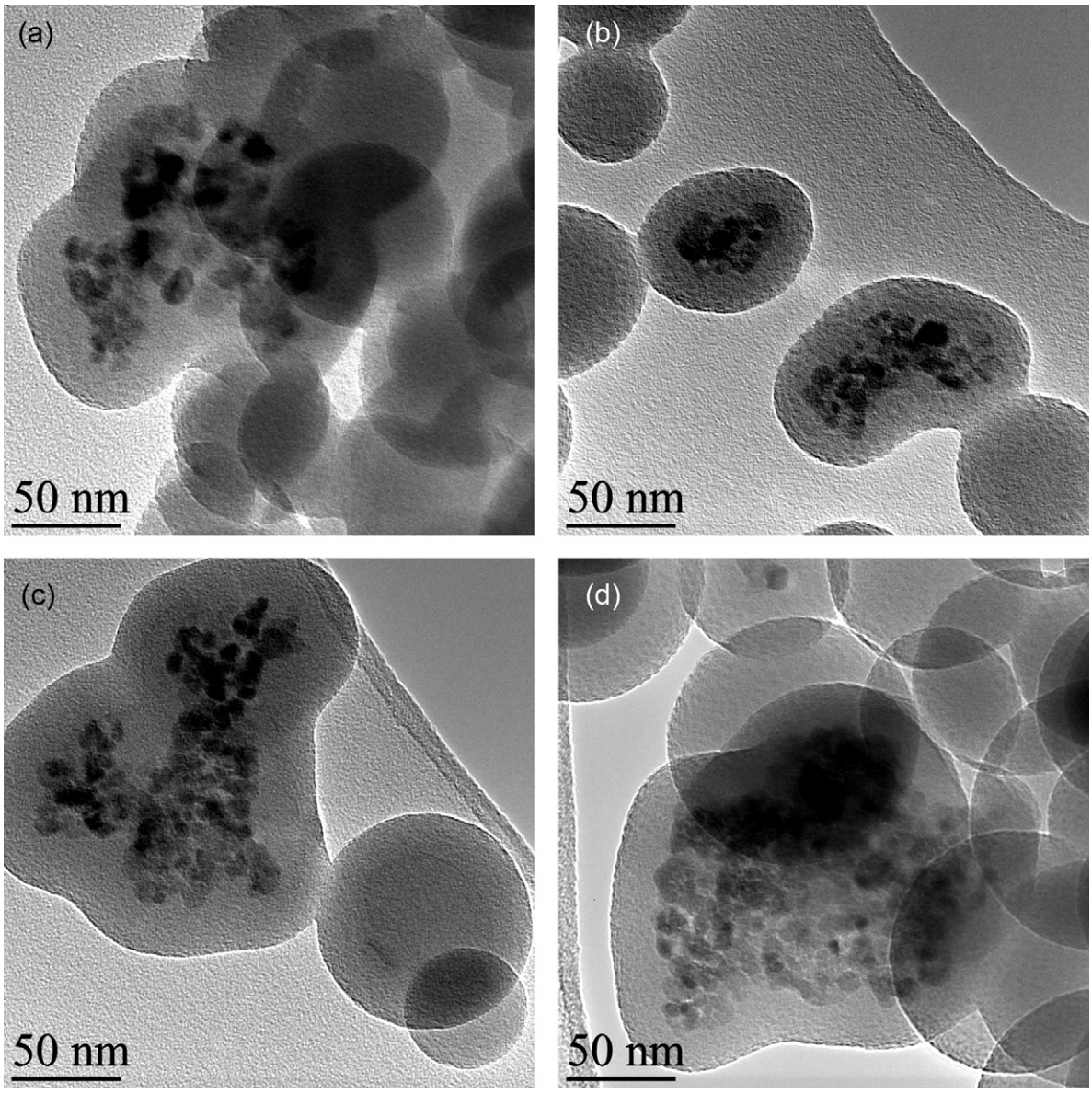

Fig. 1. TEM images of iron oxide silica-coreshell powders with (a) 0.02, (b) 0.09, (c) 0.18 and (d) 0.31 mol% Fe_3O_4.

transparent ceramics.[12] Mayerhöfer et al.[13] have compacted a transparent glass by PECS from commercial silica nanopowders, which were not fabricated via Stöber method. Thus, the present study presents new exploration of the changes in the amorphous coreshell silica with magnetic nanoparticle cores during the PECS process and the properties of the compacts.

2. Experimental

2.1. Preparation of the powder

Synthesis of iron oxide nanoparticles consisted of a simple process in ambient environment.[1] The base solution was prepared by adding 50 ml of ammonium hydroxide (NH_4OH, 25%) into 50 ml distilled water (pH 13). Iron salt precursor solution was prepared separately by dissolving 0.695 g of ferrous sulphate ($FeSO_4{\cdot}7H_2O$) in 50 ml of distilled water by using an ultrasonic agitation. Then, the iron salt solution was mixed into the base solution under magnetic stirring for 1 h. The black solution was washed twice with ethanol to remove excess ammonia, and dispersed in deionized water to its original volume.

The iron oxide–silica coreshell particles were prepared via a modified Stöber process.[14] 1160 ml of ethanol (98%), 280 ml of deionized water, and 35 ml of NH_4OH solution were mechanically stirred for 5 min before addition of 7 ml of tetraethylorthosilicate (TEOS). After 20 min, 0.02, 0.09, 0.18 or 0.31 mol% of freshly prepared iron oxide solution was added drop-wise. After 1 h mixing, 13 ml of TEOS was added and the mechanical stirring was continued for 12 h. The obtained product was dried in air and annealed at 573 K for 75 min to remove the moisture and organic compounds. Pure SiO_2 powder was also prepared for reference.

Please cite this article in press as: Mahmed N, et al. Novel iron oxide–silica coreshell powders compacted by using pulsed electric current sintering: Optical and magnetic properties. *J. Eur. Ceram. Soc.* (2012), doi:10.1016/j.jeurceramsoc.2012.02.050

2.2. Sintering and characterization

For the PECS compaction, a sample with 2.2 g of powder covered with graphite foils was put into a graphite mould with 20 mm of inner diameter. Sintering was carried out with the FCT HPD 25-2 equipment at 1323 K for 30 min in vacuum by applying pressure of 50 MPa. The thickness of the consolidated bulk samples was 2 mm. The surfaces of these samples were ground up to 1200 mesh. The phases of the materials were determined with XRD (Philips PW1710) over a 2θ range of 10–90° using Cu Kα ($\lambda = 1.5046$ Å). The morphologies of the powders and compacts were studied by transmission electron microscope (TEM Tecnai F20 200 kV) and scanning electron microscope (SEM Hitachi S-4700). The densities of the compacts (ρ) were measured with the Archimedes method in distilled water. These values were applied for determining the molar volume (V_m) of the compacted samples by $V_m = (M_T \times \text{mole fraction})/\rho$, where M_T is the total molar mass of the components. Quantum Design PPMS and Vibrating sample magnetometer (VSM PAR – Lakeshore) were used to measure the magnetic properties. The transparency of the bulk samples was studied with the UV–visible spectrometer (Perkin Elmer Lambda 950) in total transmission mode over the wavelength range of 250–800 nm. The final thickness of all the samples for the transparency study was about 1.7 mm.

3. Results and discussion

The morphologies of the powders can be observed from the TEM images in Fig. 1a–d, showing four different samples with different iron oxide contents (mol%). In these powders, the iron oxide nanoparticles are inside the silica shell forming the coreshell structures. The iron oxide nanoparticles agglomerated inside the silica structure and these agglomerates are bigger with higher amount of iron oxide. The XRD study (Fig. 2a) confirmed that the iron oxide phase in the powders B, C and D is the magnetite, Fe_3O_4 (Pdf 01-008-8148). However, in the powder A, no reflections of magnetite can be observed probably because of the very low amount of iron oxide. According to the Scherrer equation using the most intense peak (3 1 1) of XRD curves for samples B, C and D, the average size of iron oxide nanoparticles is 14 nm. The average diameter of the SiO_2 particles in the powders is about 100–250 nm determined from the TEM images by using Digital Micrograph software. As the iron oxide particles have smaller size than the wavelength of the visible light, the bulk material is expected to be transparent when consolidation takes place at the densification temperature of SiO_2.

Based on the density measurement, the Archimedes densities of the compacted samples increased with the iron oxide content from 2.18 to 2.29 g/cm^3. This is partly explained with the fact that magnetite has higher atomic weight than silica. Nevertheless, these Archimedes density values are also used in determining the V_m of the samples (Fig. 3). In the glass-component systems, V_m is used to indicate the structural changes in the glass network. Such changes take place through the formation or modification processes as the molar contents of oxides change and, thus, V_m decreases when the density of the

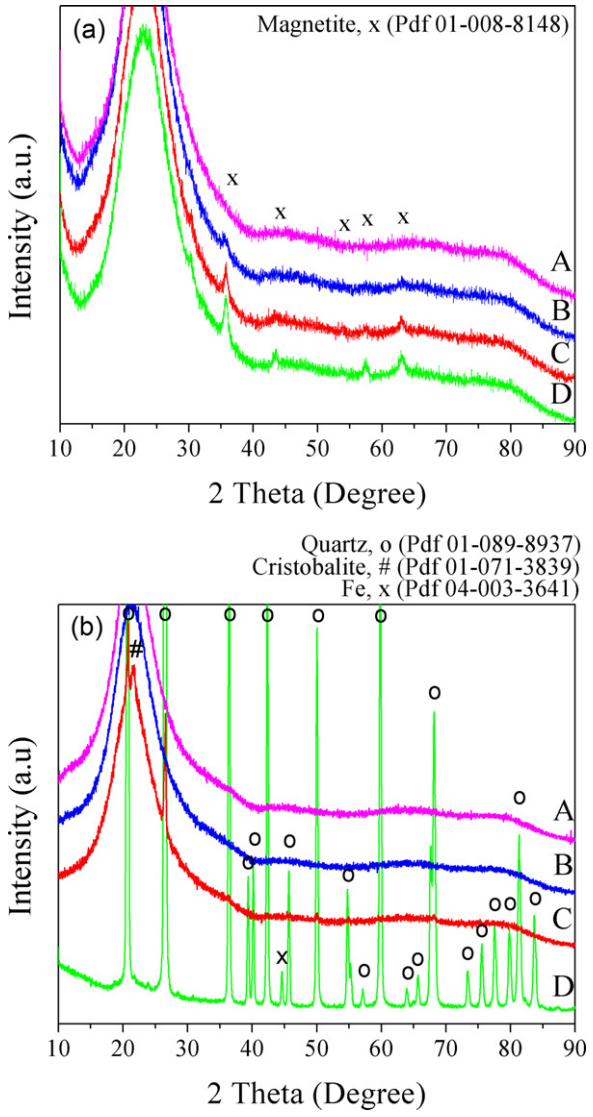

Fig. 2. XRD patterns of (a) the as-prepared powders and (b) bulk compacts with varying Fe_3O_4 content (mol%): (A) 0.02, (B) 0.09, (C) 0.18 and (D) 0.31.

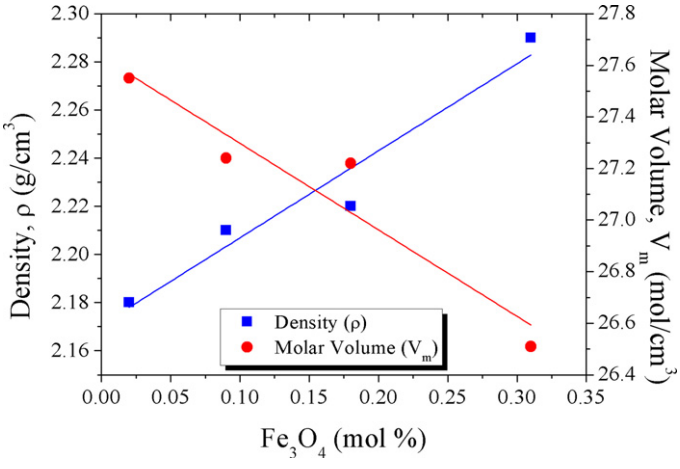

Fig. 3. Density and molar volume of the compacted samples as a function of iron oxide content of the powder (mol%).

Please cite this article in press as: Mahmed N, et al. Novel iron oxide–silica coreshell powders compacted by using pulsed electric current sintering: Optical and magnetic properties. *J. Eur. Ceram. Soc.* (2012), doi:10.1016/j.jeurceramsoc.2012.02.050

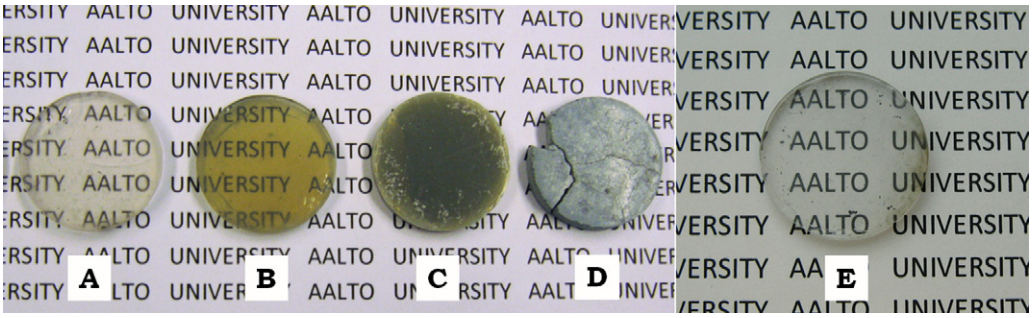

Fig. 4. The PECS compacted iron oxide–silica samples containing Fe_3O_4 (in mol%): (A) 0.02, (B) 0.09, (C) 0.18, (D) 0.31 and (E) 0. (For interpretation of the references to colour in this figure legend, the reader is referred to the web version of the article.)

glass component increases.[15] In the present case, the measured Archimedes densities of the compacted samples increase with the iron oxide content and as expected, the V_m decreases. This may be caused by the increasing amount of the non-bridging oxygen (NBO)[15] i.e. Si–O–Fe^{2+} and Si–O–Fe^{3+}, with higher iron oxide content, which suggest that both Fe^{2+} and Fe^{3+} behave as a network modifying ions.[16,17] These ions occupy the interstitial space of amorphous SiO_2 network and reduce the crystallization energy, thus promoting the crystallization at lower temperature.[17,18]

This approach is in correspondence with the XRD results of the bulk compacts in Fig. 2b. For the sintered sample of pure SiO_2, only a broad amorphous peak of silica appeared in the XRD study (not shown) indicating that amorphous structure was maintained in consolidation at 1323 K. This is consistent with the fact that the glass transition temperature of SiO_2 is about 1600 K. Similarly, the compacts made of the powders with 0.02 mol% and 0.09 mol% of iron oxide retained the amorphous structure. Their XRD patterns do not exhibit any peaks of the crystallized silica or iron oxide. The latter one may be due to the dilution of small iron content in the glassy compacts. In the XRD curve of the bulk sample C made of powder with 0.18% of iron oxide, there are no iron peaks, but some tiny peaks connected to quartz are visible at 20.8° (1 0 0) and 26.6° (0 1 1) (Pdf 01-089-8937). Thus, it can be concluded that the compact C has partially crystallized silica structure, though the major part of the silica is still amorphous. In the bulk sample D where the powder applied contained 0.31 mol% Fe_3O_4, most of the amorphous silica has transformed to quartz, and in the XRD pattern the amorphous silica hump disappears and full set of the quartz peaks appear (Fig. 2(b) – D). Furthermore, there is a Fe peak at 44.6° (1 1 0) (Pdf 04-003-3641) indicating that the iron oxide in the SiO_2 matrix has been reduced during the sintering process. The crystallization of the quartz and reduction of iron oxide during the PECS processing can be assumed by the mechanism explained below.

The coreshell powders were sintered under vacuum level of 15 Pa in which the oxygen partial pressure, $p(O_2)$ is about 3.15×10^{-5} atm. Several studies[10,11] reported that sintering under vacuum with graphite sheet/die had induced a strong reducing atmosphere around the powder to be sintered during the PECS process. Based on the Ellingham diagram,[19] the equilibrium partial pressure of oxygen for oxidation of carbon into carbon monoxide is in the range from 10^{-18} to 10^{-20} atm. The lower $p(O_2)$ equilibrium than $p(O_2)$ in vacuum causes the graphite to oxidize and producing CO (i.e., reducing environment) during the sintering process (since carbon is more stable than iron oxide) and the reduction reaction can be described by the Eq. (1) below:

$$1/2O_2 + C \leftrightarrow CO \quad (1)$$

Such a strong reducing environment during the PECS process might reduce the Fe_3O_4 nanoparticles into metallic Fe and the Fe^{3+} and Fe^{2+} ions. These ions remain in the SiO_2 network and depending on their amount they affect the glass structure as described above. Furthermore, the reducing atmosphere also has influence on the redox behaviour of the glass melt by reducing further part of the Fe^{3+} ions into Fe^{2+}.[20] Guglielmi et al.[21] reported that Fe^{2+} has a major influence upon the crystallization process of silica but it does not affect the internal nucleation which is induced by the Fe^{3+} ions, i.e. crystallization occurs only if both ferric and ferrous ions are present. With a sufficient amount of nucleating agent, the crystal growth should be catalysed by higher amount of Fe^{2+} ions.[21,22] This is in agreement with the present XRD results of the samples C and D as the crystallization is enhanced with higher amount of iron oxides in the original powder promoting perhaps more Fe^{2+} ion formation. A small cristobalite bump can be observed at 21.7° (1 1 1), (Pdf 00-027-0605) in sample C, in agreement with the report by Nanri et al.[23] whom noticed that small amount of cristobalite also formed with the existence of Fe^{2+} ions at a temperature as low as 1323 K.

As the described above, the iron oxide contents have strongly influence the stability of amorphous silica during the sintering, which finally affect the physical appearance of the samples after the consolidation process as shown in Fig. 4. When the powder contained of 0.02% of iron oxide (A), the colour of the consolidated sample is slightly yellow. The yellowish colour becomes more intense, and still maintaining its transparency when the powder containing 0.09% of iron oxide was used for compaction (B). However, when the iron oxide content increased to 0.18% (C), the olive green sample was only translucent. With further increment of the iron oxide amount that is 0.31% (D), a bluish opaque sample was obtained. Sample E made of pure SiO_2 (E) is colourless and transparent.

Please cite this article in press as: Mahmed N, et al. Novel iron oxide–silica coreshell powders compacted by using pulsed electric current sintering: Optical and magnetic properties. *J. Eur. Ceram. Soc.* (2012), doi:10.1016/j.jeurceramsoc.2012.02.050

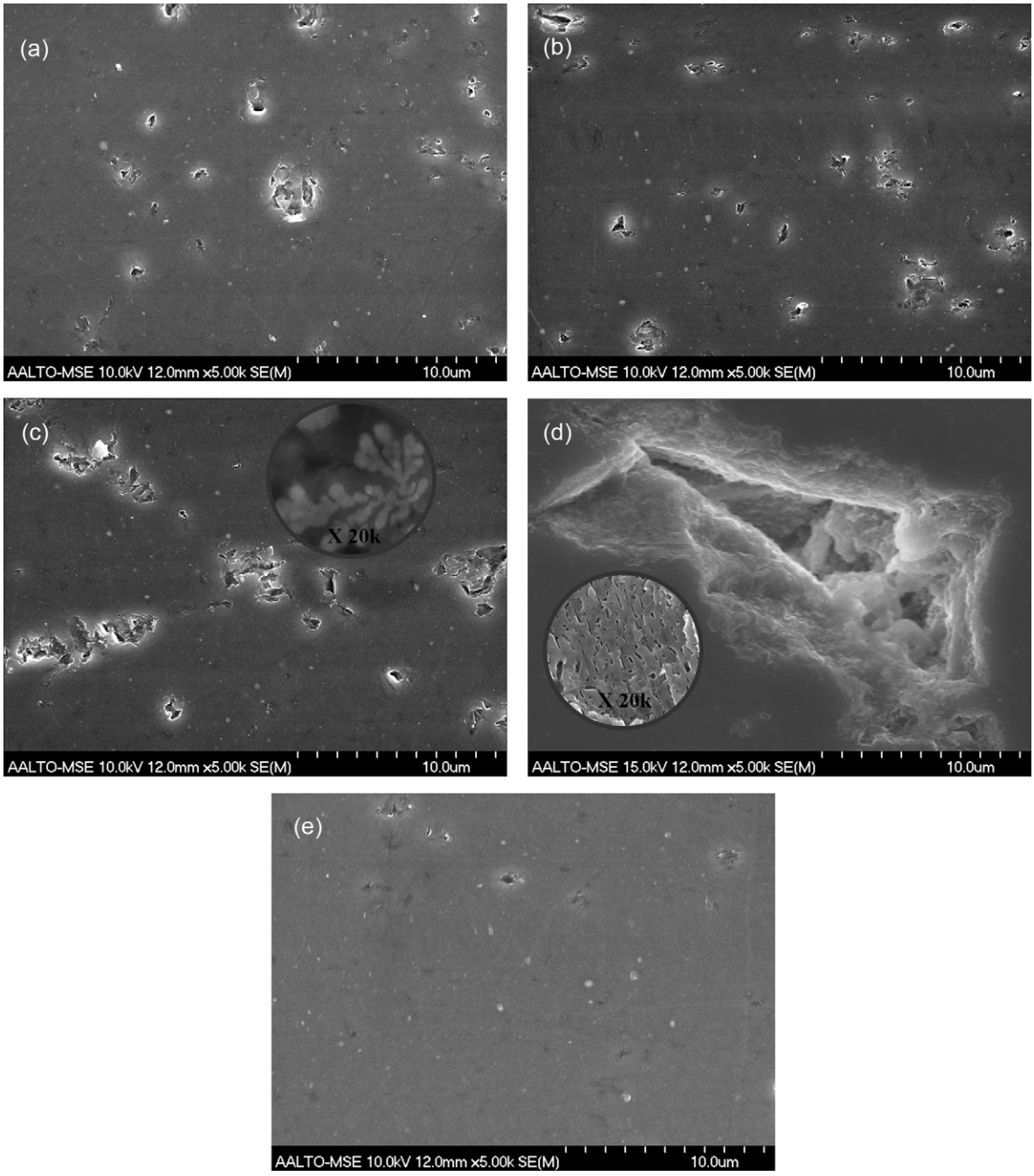

Fig. 5. SEM cross-section images of the compacted samples made of the powders with (a) 0.02, (b) 0.09, (c) 0.18, (d) 0.31 and (e) 0 mol% Fe_3O_4.

The SEM images of the cross-sections of the polished compacted samples in Fig. 5 reveal a dense microstructure for the samples A and B (Fig. 5a and b) in which the iron content is too low for inducing the crystallization of silica. However, some porosity can be observed in both of the samples. In sample C, the porosity becomes more pronounced as the amorphous glass starts to crystallize. Crystallization can be detected in the XRD curve in Fig. 2b, and it can also be observed in the SEM image of the fractured sample C (inset Fig. 5c), where dendrites with an average arm (size or) spacing of 1.2 μm, start to appear. The highest amount of iron oxide in the starting powder of the compacted sample D resulted in the growth of quartz crystals to an average size of 3.8 μm (inset Fig. 5d) well above the wavelength of the visible light, 300–800 nm, with columnar morphologies (observed from fracture surface). Large pores more than 10 μm in size can be observed in the polished sample D in Fig. 5d indicating that crystallization occurred rapidly and prevented the full densification of the sample. Fig. 5e illustrates the polished surface of iron oxide-free silica starting powder after the consolidation process with dense structure and very small porosity. The percentage of the porosities for samples A–E was estimated based on the SEM images by measuring the area of the pores. It was found that the porosity increased with increasing amount of iron oxide in the starting powder used. Porosities determined

Please cite this article in press as: Mahmed N, et al. Novel iron oxide–silica coreshell powders compacted by using pulsed electric current sintering: Optical and magnetic properties. *J. Eur. Ceram. Soc.* (2012), doi:10.1016/j.jeurceramsoc.2012.02.050

by image analysis from the polished cross-sections were 0.31% for sample A, 0.44% for sample B, and 1.9% for sample C. The porosity of sample D was highest about 42.3%, while sample E had the lowest porosity value of about 0.05%. Since the amorphous compacts also exhibit pores, the porosity is assumed to be arising due to the agglomeration of the starting powder as the iron oxide nanoparticles concentration is increased. As can be seen in the TEM images in Fig. 1, the agglomeration of the hybrid composite becomes greater with the increasing amount of iron oxide nanoparticles.

Fig. 6 shows the transmittance curves of the compacted samples in the wavelength range of 250–800 nm. The transmittance of the amorphous silica compact is 60–70% in the visible range and about 20% lower than the commercial home window that has about 92% of transparency. There are many factors that can cause to the loss of transparency in silica compact. Based on SEM image (Fig. 5e), a small number of pores can observed in the dense microstructure, together with a very small amount of residual silica particles that appeared as white dots in the image. This condition causes scattering of light and lowered the transmission of light through the sample. Other factor that might influence the transmittance of the compact is the hydroxyl groups (OH) that formed on the outer surface of the silica particles after the Stöber synthesis. These OH groups were reported to be enhanced after the PECS process.[13] It is known that the OH group is one of the main technological impurities that cause additional optical losses in the glass sample. Thus, the presence of OH groups in the consolidated sample might give rise to the absorption peak and caused the transmission loss occurred. It is known that loss of transparency may also result from the inclusions of the amorphous carbon inside the silica glass due to it permeation into the

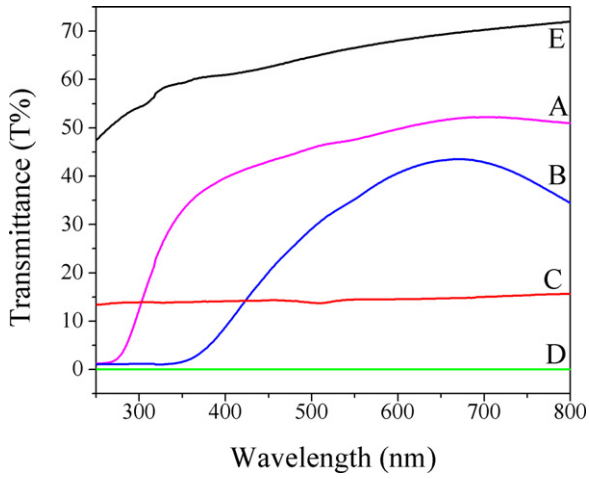

Fig. 6. UV–Vis transmittance curves of the compacted samples made of the powders with Fe_3O_4 (in mol%): (A) 0.02, (B) 0.09, (C) 0.18, (D) 0.31 and (E) 0.

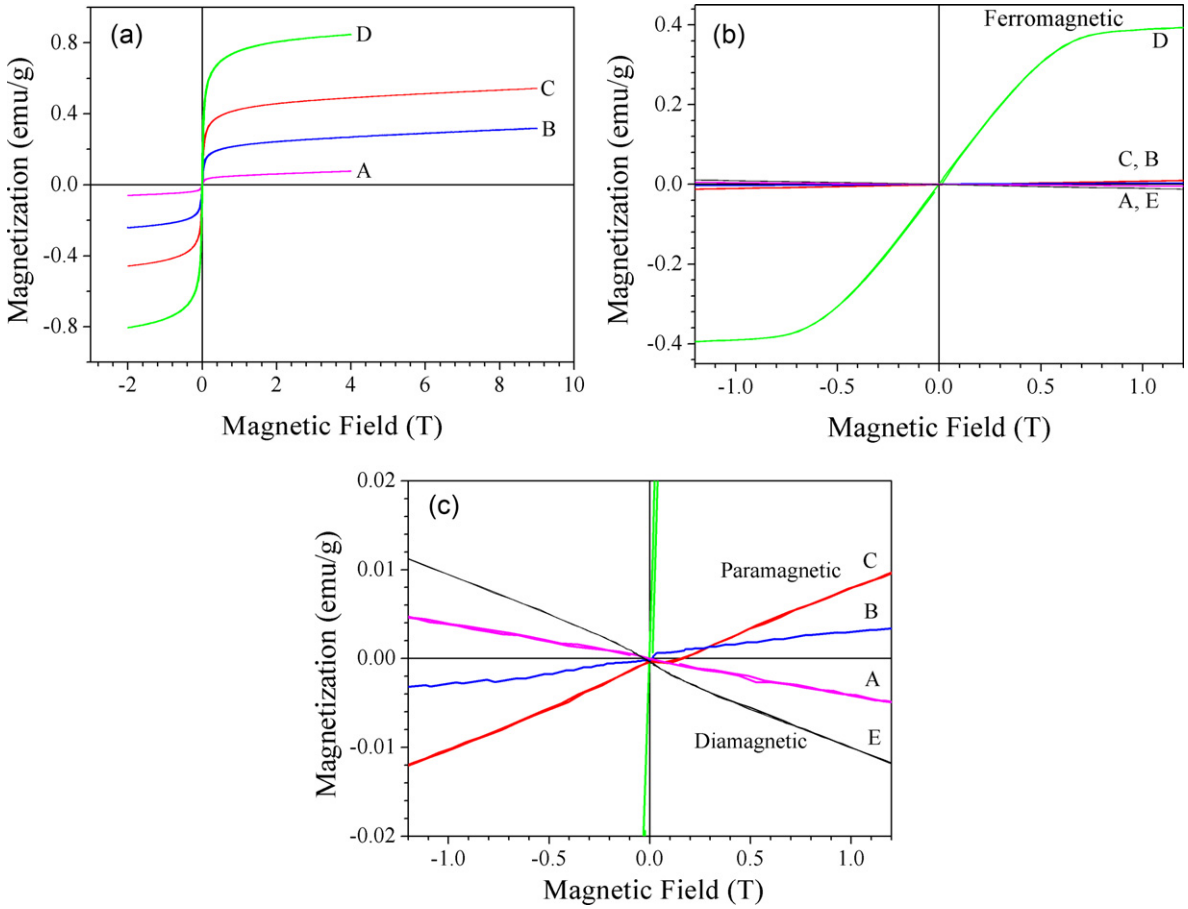

Fig. 7. Magnetic behaviour of (a) the as-prepared powders containing Fe_3O_4 (in mol%): (A) 0.02, (B) 0.09, (C) 0.18 and (D) 0.31; and the respective bulk compact (b). In (c) the magnetization of the compacted samples are shown in detail.

Please cite this article in press as: Mahmed N, et al. Novel iron oxide–silica coreshell powders compacted by using pulsed electric current sintering: Optical and magnetic properties. *J. Eur. Ceram. Soc.* (2012), doi:10.1016/j.jeurceramsoc.2012.02.050

matrix during the sintering.[13] The transparency of silica compact decreased as the iron oxide nanoparticles were inserted into the starting powder (samples A and B) and the absorption edge became broader with the powders containing higher amount of iron oxide. The loss of transparency into the translucency of sample C and opacity of the sample D is due to the devitrification of SiO_2 grains and microporosity. They act as light scattering source in the structure.[24]

The effect of the consolidation process on the room temperature magnetization of the as-prepared powders is shown in Fig. 7a. All the powders exhibit a ferromagnetic behaviour. The saturation magnetization increased approximately linearly with the higher molar composition of iron oxide in the coreshell powders. The values are correspondingly low 0.076–0.85 emu/g compared to that of the pure iron-oxide particles, 55 emu/g[1] due to the small fraction of iron oxide (less than 1 mol%) in amorphous silica matrix. However, the magnetic behaviour of the compacted bulk samples is markedly different from the powders (Fig. 7b and c). This corroborates the suggested reduction of the iron oxide phase to iron and iron ions, together with the changing of Fe^{2+}/Fe^{3+} ratio during the sintering. Sample A exhibited a diamagnetic behaviour similar with the glass sample (sample E) but with lower diamagnetic slope. This is caused by distributed iron ions, which are paramagnetic, inside the diamagnetic glassy structure. Samples B and C exhibited paramagnetic behaviour. The slope of magnetization (susceptibility) increases with increasing molar fraction of paramagnetic Fe ions. This paramagnetic behaviour can be explained by the 'shielding' or frustration of the exchange interaction between metal ions due to the random nature of glass matrix[25] and large distance between iron ions. Sample D is clearly ferromagnetic but with lower saturation magnetization (0.4 emu/g) (Fig. 7b) compared to the corresponding powder. The onset of ferromagnetic behaviour can be ascribed to the agglomeration of pure Fe clusters in compacted structure as confirmed by XRD.

The transparent (sample B) and opaque (sample D) were measured in detail at low temperature close to 0 K in order to establish the nature of the magnetic interaction from the differences in magnetic behaviour. As it is shown in Fig. 8a, both samples exhibit an increase of the magnetization at 10 K. At this temperature, a strong paramagnetic contribution appears in sample D and moreover the slope of the curve at higher field is comparable with the paramagnetic slope of sample B. This behaviour is hidden at room temperature by the major ferromagnetic part of the sample and only weak paramagnetic dependence on the field. The strong paramagnetic slope apart of ferromagnetic magnetization curve indicates that there is not only pure Fe clusters as found by XRD, which exhibits ferromagnetic interaction, but also there is similar amount of distributed paramagnetic iron ions as in the sample B. Some contribution to observed ferromagnetic behaviour might also come from the undensified part of the compact (SEM image in Fig. 5e) since the powder is ferromagnetic while the contribution to the paramagnetic behaviour might come from the glassy part of the sample in agreement with samples B and C. Magnetization as a function of temperature at 100 Oe (Fig. 8b) showed paramagnetic enhancement

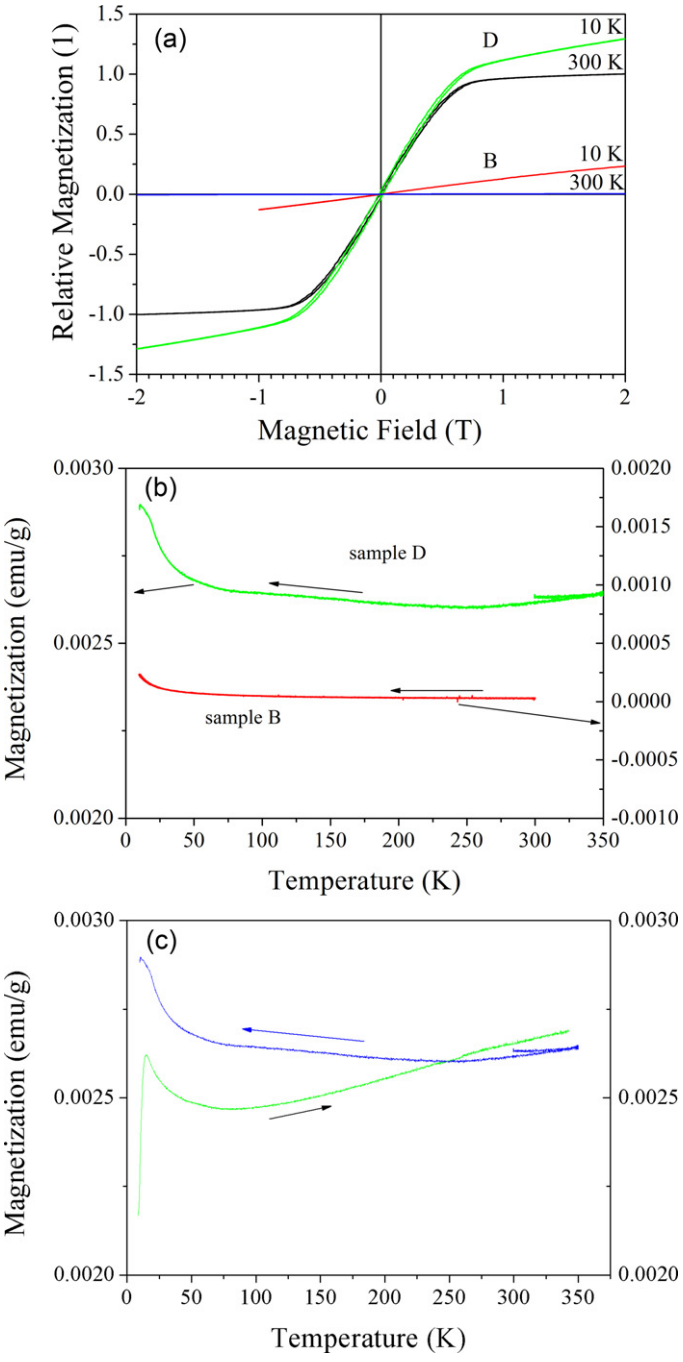

Fig. 8. Magnetic measurement of samples B and D (a) at 10 K, (b) magnetization as function of temperature and (c) cool heating of sample D.

at lower temperature for both compacts in agreement with the previous result. However, the behaviour of sample D during zero field cooling, i.e. the decrease of the magnetization at very low temperature (Fig. 8c) suggests the presence of some antiferromagnetic coupling below 10 K, too. This might be due to creation of network of iron ions with indirect exchange.

To summarize, the transparent samples were diamagnetic or paramagnetic. With increasing the iron oxide content in the powder the sample became ferromagnetic. However, the iron oxide redox reactions during the sintering process enhance the partial

Please cite this article in press as: Mahmed N, et al. Novel iron oxide–silica coreshell powders compacted by using pulsed electric current sintering: Optical and magnetic properties. *J. Eur. Ceram. Soc.* (2012), doi:10.1016/j.jeurceramsoc.2012.02.050

or full crystallization of the silica, resulting in translucent or opaque material and the presence of pure Fe. In order to obtain transparent ferromagnetic material, the processing parameters should be optimized and redox reaction suppressed.

4. Conclusion

Transparent bulk magnetic compacts were produced by the PECS method from the iron oxide–silica coreshell powders prepared by Stöber method. Increasing the amount of iron oxide content in the coreshell powders induced the crystallization of the amorphous silica glass and microporosity formation during the sintering process. Because of microporosity and the partially undensified parts of the compacted sample, as well as the grain size of the crystallize silica larger than wavelength of visible light, light scattering and loss of transparency occurred. The reduction of the iron oxide to metallic iron and iron ions during the sintering process promoted the ferromagnetism in the materials with higher Fe content. Ferromagnetic transparent material might be obtained if the grain growth, microporosities and full density of the compact can be achieved by optimization of the sintering parameters. A promising magnetic property of the transparent or translucent compacted samples might have a good potential in magneto-optical studies.

Acknowledgements

Graduate School of Advanced Materials and Processes at the Aalto University Finland and OPNA-project funded by the Academy of Finland are thanked for support.

References

1. Mahmed N, Heczko O, Söderberg O, Hannula S-P. Room temperature synthesis of magnetite ($Fe_{3-\delta}O_4$) nanoparticles by a simple reverse co-precipitation method. *IOP Conf Ser Mater Sci Eng* 2011;**18**:032020.
2. Guardia P, Batlle-Brugal B, Roca AG, Iglesias O, Morales MP, Serna CJ, et al. Surfactant effects in magnetite nanoparticles of controlled size. *J Magn Magn Mater* 2007;**316**:756–9.
3. Kura H, Takahashi M, Ogawa T. Synthesis of monodisperse iron nanoparticles with a high saturation magnetization using an Fe(CO)x-oleylamine reacted precursor. *J Phys Chem C* 2010;**114**:5835–8.
4. Bahuguna R, Mina M, Tioh J-W, Weber RJ. Magneto-optic-based fiber switch for optical communications. *IEEE Trans Magn* 2006;**42**:3099–101.
5. Krumme J-P, Heitmann H, Mateika D, Witter K. MOPS, a magneto-optic-photoconductor sandwich for optical information storage. *J Appl Phys* 1977;**48**:366–8.
6. Zamani M, Ghanaatshoar M, Alisafaee H. Adjustable magneto-optical isolators with high transmittance and large Faraday rotation. *J Opt Soc Am B* 2011;**28**:2637–42.
7. Yamaguchi K, Matsumoto K, Fujii T. Magnetic anisotropy by ferromagnetic particles alignment in a magnetic field. *J Appl Phys* 1990;**67**:4493–5.
8. Yasumori A, Matsumoto H, Hayashi S, Okada K. Magneto-optical properties of silica gel containing magnetite fine particle. *J Sol-Gel Sci Technol* 2000;**18**:249–58.
9. Thomas S, Sakthikumar D, Joy PA, Yoshida Y, Anantharaman MR. Optically transparent magnetic nanocomposite based on encapsulated Fe_3O_4 nanoparticles in a sol–gel silica network. *Nanotechnology* 2006;**17**:5565–73.
10. Ran S, Vleugels J, Huang S, Vanmeensel K, Blank DHA, Winnubst L. Manipulating microstructure and mechanical properties of CuO doped 3Y-TZP nano-ceramics using spark plasma sintering. *J Eur Ceram Soc* 2010;**30**:899–904.
11. Yoon S, Dornseiffer J, Xiong Y, Gruner D, Shen Z, Iwaya S, et al. Synthesis, spark plasma sintering and electrical conduction mechanism in $BaTiO_3$–Cu composite. *J Eur Ceram Soc* 2011;**31**:773–82.
12. Wang C, Zhao Z. Transparent $MgAL_2O$ ceramic produced by spark plasma sintering. *Scripta Mater* 2009;**61**:193–6.
13. Mayerhöfer TG, Shen Z, Leonova E, Eden M, Kriltz A, Popp J. Consolidate silica glass from nanoparticles. *J Solid State Chem* 2008;**181**:2442–7.
14. Lu Z, Dai J, Song X, Wang G, Yang W. Facile synthesis of Fe_3O_4/SiO_2 composite nanoparticles from primary silica particles. *Colloids Surf A* 2008;**317**:450–6.
15. El-Hadi ZA, Farouk H, Khalifa FA, Moustaffa FA. Molar volume of some sodium silicate and sodium borosilicate glasses. *Commun Fac Sci Univ Ank Ser B* 1991;**31**:49–57.
16. Mekki A, Holland D, Ziq KA, McConville CF. Structural and magnetic properties of sodium iron germanate glasses. *J Non-Cryst Solids* 2000;**272**:179–90.
17. Salama SN, Salman SM. Crystallization characteristics of iron-containing spodumene-dopside glasses. *J Eur Ceram Soc* 1993;**12**:61–9.
18. Wang S. Effects of Fe on crystallization and properties of a new high infrared radiance glass-ceramics. *Environ Sci Technol* 2010;**44**:4816–20.
19. Ellingham HJT. Reducibility of oxides and sulfides in metallurgical processes. *J Soc Chem Ind* 1994;**63**:125–33.
20. Zehani K, Mazaleyrat F, Loyau V, Labouré E. Effect of temperature and time on properties of spark plasma sintered NiCuZn:Co ferrite. *J Appl Phys* 2011;**109**:07A504.
21. Guglielmi M, Mashio RD, Molinari A. Crystallization of silica in SiO_2–Fe_2O_3 glasses obtained from gels. *Mater Chem Phys* 1985;**13**:171–7.
22. Lonnroth N, Yue YZ. Structural order and crystallization of an iron-rich aluminosilicate liquid under oxidizing condition. *J Non-Cryst Solids* 2008;**354**:1190–3.
23. Nanri H, Takeuchi N, Ishida S, Watanabe K, Wakamatsu M. Mineralizing action of iron in amorphous silica. *J Non-Cryst Solids* 1996;**203**:375–9.
24. Kim BN, Hiraga K, Morita K, Yoshida H, Miyazaki T, Kagawa Y. Microstructure and optical properties of transparent alumina. *Acta Mater* 2009;**57**:1319–26.
25. Mekki A. Magnetic properties of Fe ions in a silicate glass and ceramic. *Phys Stat Sol A* 2001;**184**:327–33.

Please cite this article in press as: Mahmed N, et al. Novel iron oxide–silica coreshell powders compacted by using pulsed electric current sintering: Optical and magnetic properties. *J. Eur. Ceram. Soc.* (2012), doi:10.1016/j.jeurceramsoc.2012.02.050